

Measurement of differential cross sections and of the Higgs boson mass in Higgs boson decays to bosons using the ATLAS detector

Antoine Laudrain*, on behalf of the ATLAS Collaboration

Johannes Gutenberg Universität, Mainz, Germany

E-mail: antoine.laudrain@cern.ch

Despite small branching fractions, the $H \rightarrow \gamma\gamma$ and $H \rightarrow ZZ^* \rightarrow 4\ell$ Higgs boson decays provide clean and well reconstructed final states, allowing for precise measurements of the Higgs boson properties. These proceedings present measurements of total and differential fiducial cross sections in the $H \rightarrow \gamma\gamma$ and $H \rightarrow ZZ^* \rightarrow 4\ell$ decay channels, and a mass measurement in the $H \rightarrow ZZ^* \rightarrow 4\ell$ decay channel. The total fiducial cross section is measured to be $\sigma_{\text{fid}}^{\gamma\gamma} = 65.2 \pm 7.1$ fb in the $H \rightarrow \gamma\gamma$ channel and $\sigma_{\text{fid}}^{4\ell} = 3.28 \pm 0.32$ fb in the $H \rightarrow ZZ^* \rightarrow 4\ell$ channel, in agreement with the Standard Model predictions. Differential cross-section measurements are reported for Higgs boson production- and decay-related observables. The Higgs boson transverse momentum differential cross-section distributions are used to constrain the charm Yukawa coupling modifier (95% confidence level interval on κ_c of $[-12, 11]$ in the $H \rightarrow 4\ell$ analysis and of $[-19, 24]$ in the $H \rightarrow \gamma\gamma$ analysis). Other differential cross-section distributions allow constraints on pseudo-observables and effective field theory coefficients. The Higgs boson mass in the $H \rightarrow ZZ^* \rightarrow 4\ell$ decay channel is measured to be $m_H = 124.92 \pm 0.19$ (stat.) $^{+0.09}_{-0.06}$ (sys.) GeV. All the results are derived using 139 fb^{-1} of $\sqrt{s} = 13$ TeV proton-proton collisions collected with the ATLAS detector during the Run 2 of the LHC.

*40th International Conference on High Energy physics - ICHEP2020
July 28 - August 6, 2020
Prague, Czech Republic (virtual meeting)*

*Speaker



1. Introduction

Higgs boson studies have achieved major milestones using partial datasets from the Run 2 of the LHC, such as the observation of the $H \rightarrow b\bar{b}$ decay and the $t\bar{t}H$ production mode, thus further confirming the predictions of the Standard Model. At the end of Run 2, the ATLAS experiment [1] has recorded 139 fb^{-1} of proton–proton collision data at $\sqrt{s} = 13 \text{ TeV}$. This unprecedented amount of data enables increasingly precise tests of the Higgs boson properties and of the Standard Model.

Despite their small branching ratios, the $H \rightarrow \gamma\gamma$ and $H \rightarrow ZZ^* \rightarrow 4\ell$ ($\ell = e, \mu$) decay channels exhibit excellent precision in a variety of analyses due to their fully reconstructed and precisely measured final states. These proceedings summarise three analyses performed in these two channels, using the full Run 2 dataset: the Higgs boson cross-section measurements in the $H \rightarrow \gamma\gamma$ [2] and $H \rightarrow ZZ^* \rightarrow 4\ell$ [3] decay channels, and the Higgs boson mass measurement in the $H \rightarrow ZZ^* \rightarrow 4\ell$ decay channel [4].

2. Fiducial and differential cross-section measurements

Fiducial and differential cross sections are one of the key measurements of the Higgs boson, as they allow for largely model-independent measurements. In these analyses, the fiducial phase space is defined to closely match the experimentally accessible phase space, therefore minimising the model-dependent extrapolations. Observables are then chosen regarding their ability to probe various kinematics of the Higgs boson production and decay. For example, the Higgs transverse momentum is sensitive to the charm and bottom quarks Yukawa couplings in Higgs boson production, while the number of jets is sensitive to the fraction of each Higgs boson production mechanisms and angular observables in the four-lepton decay system are sensitive to the Higgs boson spin-parity. The $H \rightarrow ZZ^* \rightarrow 4\ell$ analysis defines 20 such differential fiducial observables (including eight doubly differential observables), and the preliminary $H \rightarrow \gamma\gamma$ analysis defines six such observables.

The number of signal events in each bin of each differential observable is then extracted using a fit to the di-photon ($m_{\gamma\gamma}$) or four-lepton ($m_{4\ell}$) invariant mass distribution and unfolded to the fiducial region. These two mass distributions for all events are shown in Figure 1. The total fiducial cross sections are computed in both analyses, yielding $\sigma_{\text{fid}}^{\gamma\gamma} = 65.2 \pm 4.5 \text{ (stat.)} \pm 5.6 \text{ (syst.)} \pm 0.3 \text{ (theo.) fb}$, and $\sigma_{\text{fid}}^{4\ell} = 3.28 \pm 0.32 \text{ fb}$, both compatible with the Standard Model predictions ($\sigma_{\text{fid,SM}}^{\gamma\gamma} = 63.6 \pm 3.3 \text{ fb}$ and $\sigma_{\text{fid,SM}}^{4\ell} = 3.41 \pm 0.18 \text{ fb}$, respectively). The leading systematic uncertainties in the $H \rightarrow \gamma\gamma$ analysis are the background modelling and the photon energy scale and resolution. Uncertainties of analyses in the $H \rightarrow 4\ell$ channel are statistically dominated.

The unfolded distributions are finally compared to various Monte-Carlo (MC) predictions. An example for the $p_{\text{T}}(\gamma\gamma)$ and $p_{\text{T}}(4\ell)$ distributions is shown in Figure 2. The p -values between the data and the MC predictions are computed for all unfolded distributions. No significant deviation from the Standard Model is observed.

Assuming all coupling modifiers vanish for the Standard Model value, a non-zero charm Yukawa coupling modifier (κ_c) would modify the c -quark contribution in the ggF loop, and therefore change the $p_{\text{T}}(\gamma\gamma)$ and $p_{\text{T}}(4\ell)$ distributions, particularly at low p_{T} . Using a fit on these observables, both analyses constrain κ_c , providing a 95 % confidence level interval of $[-19, 24]$ ($H \rightarrow \gamma\gamma$) and $[-12, 11]$ ($H \rightarrow 4\ell$).

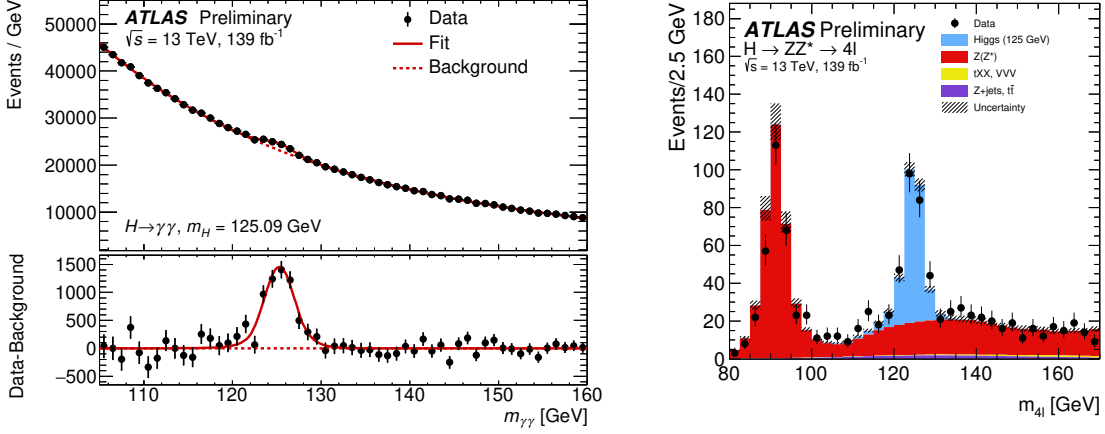


Figure 1: Di-photon (left) and four-lepton (right) invariant mass distributions used for the unfolding [2, 3].

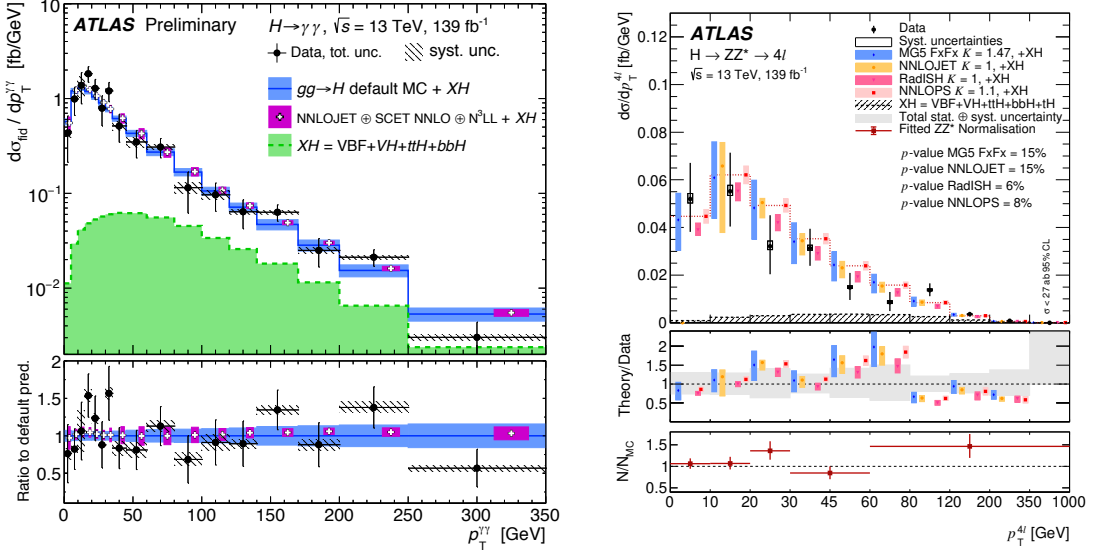


Figure 2: Unfolded $p_T(\gamma\gamma)$ (left) and $p_T(4\ell)$ (right) distributions compared to various MC predictions [2, 3].

The pseudo-observables (PO) framework [5] introduces contact terms between the Higgs boson, the Z boson, and the left- or right-handed leptons (ϵ_{Z,ℓ_L} and ϵ_{Z,ℓ_R}). Using the double differential cross section m_{Z1} vs. m_{Z2} , the $H \rightarrow 4\ell$ analysis is sensitive to these modifiers and can discriminate between Higgs– Z bosons and Z –leptons interactions. Four different scenarios were explored, assuming various symmetries, and an example is reported in Figure 3 (left). The results are compatible with the Standard Model expectation.

Effective field theories (EFT) are another commonly used framework to interpret results, as they encompass all possible new physics effects. Focusing on dimension-6 operators linked to the Higgs boson to vector boson couplings, the effective Lagrangian in the SMEFT basis reduces to

$$\begin{aligned} \mathcal{L}_{\text{eff}}^{\text{SILH}} \supset & \bar{C}_{HG} O'_{HG} + \bar{C}_{HW} O'_{HW} + \bar{C}_{HB} O'_{HB} + \bar{C}_{HWB} O'_{HWB} \\ & + \tilde{C}_{HG} \tilde{O}'_{HG} + \tilde{C}_{HW} \tilde{O}'_{HW} + \tilde{C}_{HB} \tilde{O}'_{HB} + \tilde{C}_{HWB} \tilde{O}'_{HWB} \end{aligned} \quad (1)$$

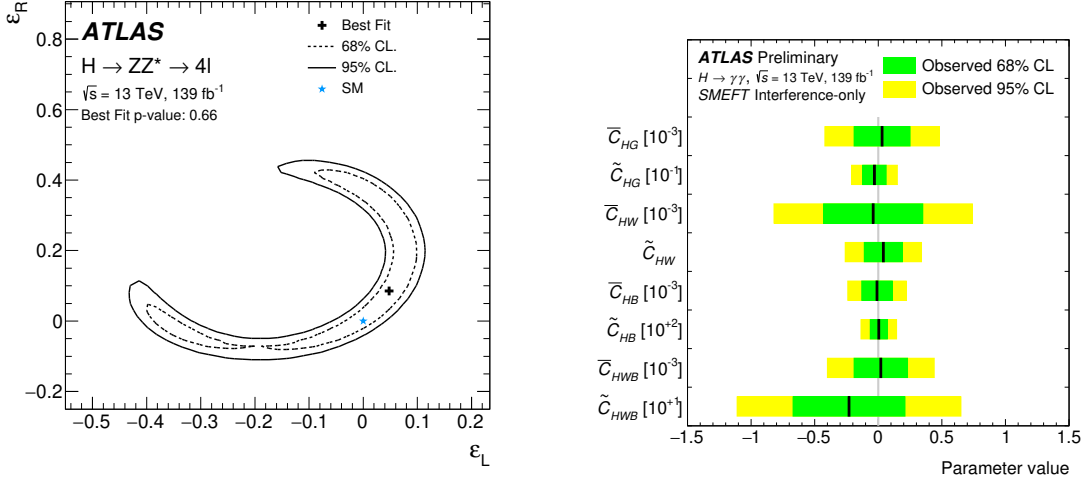


Figure 3: Example of pseudo observable limits from the $H \rightarrow 4\ell$ analysis (left) [3], and limits from a global fits to all observables expressed in the SMEFT basis (right) [2].

where the \mathcal{O} are the new interactions and the c_i the Wilson coefficients tuning their strengths. The tilde version of the operators and coefficients denote the CP-odd effects. As a non-vanishing value of a Wilson coefficient modifies the differential distribution shapes compared to the Standard Model, the $H \rightarrow \gamma\gamma$ analysis uses a combined fit to all bins of all observables to constrain the eight Wilson coefficients mentioned above (Figure 3 right). Results were reported in both the SILH and SMEFT bases, varying one coefficient at a time (all others set to 0). No significant deviation from the Standard Model expectation is seen.

3. Mass measurement

The reference Higgs boson mass is set by a combination of the measurements performed by the ATLAS and CMS experiments in the $H \rightarrow \gamma\gamma$ and $H \rightarrow ZZ^* \rightarrow 4\ell$ decays channels using the 7 and 8 TeV data recorded during the Run 1 of the LHC [6]: $m_H = 125.09 \pm 0.24 \text{ GeV}$. Given the ten fold increase in the Higgs boson decay statistics between Run 1 and Run 2, individual channels are now able to improve the precision of this reference measurement.

The $H \rightarrow 4\ell$ decay channel suffers from low statistics but benefits from a large signal to background ratio of about 2. This makes it a golden channel for the Higgs boson mass measurement. Using the full Run 2 dataset, 314 events are observed in the mass region $115 \text{ GeV} < m_{4\ell} < 130 \text{ GeV}$, for 316 expected events. On top of the increased statistics, several methods are employed to improve the precision of the result. The four main ones used in this analysis are recalled below, the last having been a recent development [4].

First, the photons emitted through final state radiations (FSR) are looked for and included in the kinematics of the four-lepton system. This FSR recovery impacts 4 % of events, and improves the mass resolution by about 1 %.

Second, the mass of the leading di-lepton pair is constrained to the Z boson mass using a kinematic fit, bringing a 17 % improvement to the four-lepton mass resolution.

Third, a boosted decision tree (BDT) is trained to discriminate the $H \rightarrow ZZ^* \rightarrow 4\ell$ signal from the $q\bar{q} \rightarrow ZZ^*$ background. The transverse momentum and pseudorapidity of the four lepton-system and a kinematic discriminant based on a matrix-element likelihood for the $gg \rightarrow H \rightarrow 4\ell$ and $q\bar{q}/gg \rightarrow ZZ^*$ processes are used as discriminating variables. The analysis is performed simultaneously over four bins of this BDT for each of the 4μ , $2\mu 2e$, $2e 2\mu$ and $4e$ final states, for a total of 16 categories. This improves the resolution by about 2%.^o

Fourth, the $m_{4\ell}$ line shape is modelled by a double-sided Crystal-Ball distribution (DSCB), and its resolution is computed on an event-per-event basis:

$$\text{DSCB}(m_{4\ell}; \mu, \kappa \times \sigma_i, \alpha_1, n_1, \alpha_2, n_2 | \sigma_i), \quad (2)$$

where μ is the mean of the gaussian core, α_k and n_k the tail parameters, and σ_i the resolution for the event i (κ absorbs the data/MC differences). One such DSCB is independently defined in each analysis category. The per-event resolution parameter σ_i is predicted using a quantile-regression neural network (QRNN), trained on the individual lepton kinematics (p_T, η, ϕ) and the four-lepton system momentum, as well as their uncertainties. The distribution of expected and observed σ_i as well as the combined fit over all analyses categories are shown in Figure 4.

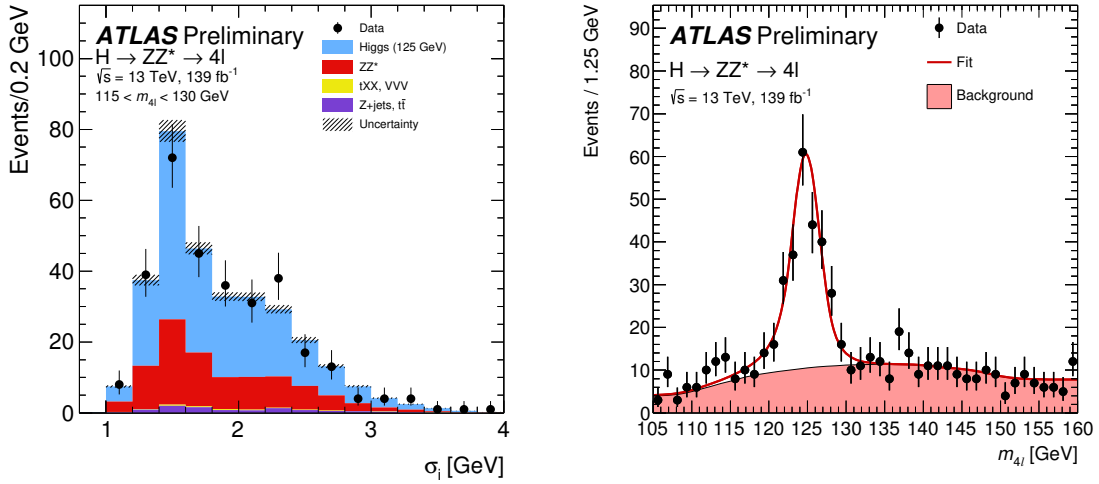


Figure 4: Expected and observed event-level resolution σ_i predicted by the QRNN (left), and combined $m_{4\ell}$ fit over all 16 analysis categories (right) [4].

The combined fit to all categories yields a Higgs boson mass of

$$m_H^{4\ell} = 124.92 \pm 0.19 \text{ (stat.)}_{-0.06}^{+0.09} \text{ (sys.) GeV} = 124.92_{-0.20}^{+0.21} \text{ GeV}. \quad (3)$$

A good agreement between the 4μ , $2\mu 2e$, $2e 2\mu$ and $4e$ final states is found. The result improves a previous ATLAS result combining Run 1 and early Run 2 data in the $H \rightarrow 4\ell$ and $H \rightarrow \gamma\gamma$ channels [7] by 15%, and is also compatible with an analogue $H \rightarrow 4\ell$ result from CMS using 36 fb^{-1} of Run 2 data [8]: $m_H^{4\ell, \text{CMS}} = 125.26 \pm 0.21 \text{ GeV}$. While the uncertainty is still mainly coming from the statistical component, the systematic uncertainties are dominated by the muon momentum scale ($_{-0.06}^{+0.08} \text{ GeV}$).

4. Summary

Fiducial cross-sections results from the $H \rightarrow \gamma\gamma$ and $H \rightarrow ZZ^* \rightarrow 4\ell$ analyses using the full Run 2 dataset are reported. The total fiducial cross sections are measured to be $\sigma_{\text{fid}}^{\gamma\gamma} = 65.2 \pm 7.1$ fb and $\sigma_{\text{fid}}^{4\ell} = 3.28 \pm 0.32$ fb, in agreement with the Standard Model predictions of $\sigma_{\text{fid,SM}}^{\gamma\gamma} = 63.6 \pm 3.3$ fb and $\sigma_{\text{fid,SM}}^{4\ell} = 3.41 \pm 0.18$ fb, respectively. The differential fiducial measurements are used to constrain the charm Yukawa coupling modifier, yielding a 95 % confidence level interval on κ_c of $[-12, 11]$ in the $H \rightarrow 4\ell$ analysis and of $[-19, 24]$ in the $H \rightarrow \gamma\gamma$ analysis. As no significant deviation from the Standard Model is observed, the results are also interpreted in terms of limits on pseudo-observables and effective field theory coefficients.

The Higgs boson mass in the $H \rightarrow ZZ^* \rightarrow 4\ell$ decay channel is measured to be $m_H = 124.92 \pm 0.19$ (stat.) $_{-0.06}^{+0.09}$ (sys.) GeV, improving the previous ATLAS result by 15 %.

References

- [1] ATLAS Collaboration, *The ATLAS Experiment at the CERN Large Hadron Collider*, *JINST* **3** (2008) S08003.
- [2] ATLAS collaboration, *Measurements and interpretations of Higgs-boson fiducial cross sections in the diphoton decay channel using 139 fb^{-1} of pp collision data at $\sqrt{s} = 13 \text{ TeV}$ with the ATLAS detector*, Tech. Rep. [ATLAS-CONF-2019-029](#), CERN, Geneva (Jul, 2019).
- [3] ATLAS collaboration, *Measurements of the Higgs boson inclusive and differential fiducial cross sections in the 4ℓ decay channel at $\sqrt{s} = 13 \text{ TeV}$* , *Eur. Phys. J. C* **80** (2020) 942 [[2004.03969](#)].
- [4] ATLAS collaboration, *Measurement of the Higgs boson mass in the $H \rightarrow ZZ^* \rightarrow 4\ell$ decay channel with $\sqrt{s} = 13 \text{ TeV}$ pp collisions using the ATLAS detector at the LHC*, Tech. Rep. [ATLAS-CONF-2020-005](#), CERN, Geneva (Apr, 2020).
- [5] J.S. Gainer et al., *Adding pseudo-observables to the four-lepton experimentalist's toolbox*, *JHEP* **10** (2018) 073 [[1808.00965](#)].
- [6] ATLAS and CMS Collaborations, *Combined Measurement of the Higgs Boson Mass in pp Collisions at $\sqrt{s} = 7$ and 8 TeV with the ATLAS and CMS Experiments*, *Phys. Rev. Lett.* **114** (2015) 191803 [[1503.07589](#)].
- [7] ATLAS Collaboration, *Measurement of the Higgs boson mass in the $H \rightarrow ZZ^* \rightarrow 4\ell$ and $H \rightarrow \gamma\gamma$ channels with $\sqrt{s} = 13 \text{ TeV}$ pp collisions using the ATLAS detector*, *Phys. Lett. B* **784** (2018) 345 [[1806.00242](#)].
- [8] CMS Collaboration, *Measurements of properties of the Higgs boson decaying into the four-lepton final state in pp collisions at $\sqrt{s} = 13 \text{ TeV}$* , *JHEP* **11** (2017) 047 [[1706.09936](#)].